Eur. Phys. J. D **63**, 301–306 (2011)
DOI: 10.1140/epjd/e2011-10605-7

THE EUROPEAN PHYSICAL JOURNAL D

Regular Article

Gold aggregates on silica templates and decorated silica arrays for SERS applications

F. Castillo[1,a], E. De la Rosa[2], and E. Pérez[3]

[1] Doctorado en Ingeniería y Ciencia de Materiales (DICIM), Universidad Autónoma de San Luis Potosí, Av. Manuel Nava #6, Zona Universitaria, 78290 San Luis Potosí, México
[2] Centro de Investigaciones en Óptica, A.C. A.P. 1-948, León Gto., 37150, Mexico
[3] Instituto de Física, Universidad Autónoma de San Luis Potosí, Av. Manuel Nava #6, Zona Universitaria, 78290 San Luis Potosí, Mexico

Received 20 October 2010 / Received in final form 12 January 2011
Published online 9 June 2011 –

Abstract. In this work, we report the fabrication and characterization of size controllable gold nanoparticles (NPs) aggregates for their application in surface enhanced Raman scattering (SERS). Aggregates were prepared using two methodologies: (i) by using silica particles arrays as a template to agglomerate gold NPs between the inter-particle interstices, and (ii) by functionalizing silica particles to be used as support to graft gold nanoparticles and thus to form decorated silica particle arrays. These substrates were used in the detection of Rhodamine 6G producing an enhancement factor (EF) from 10^4 to 10^6 that is associated to the increment of hot spot (HS) sites, and the fact that plasmon resonance from aggregates and absorption wavelength of test molecules are closely in resonance with excitation wavelength. The EF was also reduced when the plasmon resonance was red-shifted as a result of the increment of aggregate size. In spite of this, the EF is high enough to make these SERS substrates excellent candidates for sensing applications.

1 Introduction

Surface enhanced Raman scattering (SERS) is a high sensitive spectroscopic tool for low concentration detection of analytes, including single molecule detection [1–4]. The physical mechanism associated to such enhancement has been widely studied and reported elsewhere [4–11]. The most accepted mechanism is based on the electromagnetic field (EM) enhancement due to the optical field localization on metal nanostructures, and the electronic enhancement due to the increase of Raman cross-section [12,13]. Experimental evidences and theoretical simulations indicate that maximum enhancement factor (EF) occurs when target molecules are located near a metal surface and that enhancement rapidly attenuates within a few nanometers away from the surface [14,15].

Recently, it has been reported an extremely high SERS signal ($\sim 10^{10}$) at the junction of two or more nanoparticles, such active sites named hot spot (HS) represent position of maximum enhancement of EM [16,17]. Since these reports, several efforts have been done to fabricate aggregates with well-defined junction sites.

Kneipp et al. reported strong SERS signals produced by the aggregation of gold (Au) nanoparticles (NPs) formed by the addition of sodium chloride (NaCl) to the gold solution. However, the addition of NaCl destroys the morphology of Au NPs resulting on irregular particles and poor reproducibility in the formation of aggregates [18,19]. Zhang et al. reported gold nanoparticles arrays (GNAs) obtained by using Na_2S as a reducer agent during their synthesis that produces Au NPs aggregates [20]. Aggregation process is driven by slightly variations in reagent (Na_2S) concentration. However, the GNAs produce a broad distribution of sizes and shapes inducing a broad plasmon band (600–1000 nm). As consequence, they estimated that around 1% of the aggregates are on resonance with the excitation wavelength. Therefore, a controllable synthesis of nanoparticles aggregates is actually the major goal for SERS optimization.

In this way, Wang et al. have proposed an alternative method to fabricate nanoparticles substrates by grafting Au NPs onto functionalized SiO_2 particles by using silane-coupling agents with different functional groups [21], they can control Au NPs aggregation and selective adsorption of ClO_4^- on functionalized nanoparticles substrates. These Au NPs decorated SiO_2 substrate increase the probability of finding a HS until $\sim 1/50$, which can be compared with 1/1000 using pure metallic colloids [22]. Another way to fabricate SERS substrates was proposed by Yan et al. based on the use of a PMMA mask on a glass-gold slide substrate [23]. A solution of Au NPs was deposited onto the slide, and after solvent evaporation, a 2D pattern of nanoparticles aggregates were obtained. This approach provides a control over the size of the particle aggregates

[a] e-mail: jjfcr02@gmail.com

and their spatial location on the substrate. In this case, SERS experiments show high reproducibility in different areas on the substrate and in different substrates fabricated with this approach. However, this method is limited to produce only 2D arrays.

In this work, we report the preparation and the systematic characterization of SERS response of Au NPs aggregates prepared on substrates by two methodologies: (i) a silicon slide with an arrangement of silica particles as a template to fabricate Au NPs aggregates between the inter-particle interstices, (ii) functionalized silica particles used as support for grafting Au NPs and thus forming decorated silica particle arrays. These substrates were used to study the SERS response as a function of the aggregates size. The goal of this work is to extend the already existing methodologies to control the size and shape of aggregates for applications as SERS substrates and to analyze the resonant conditions imposed by a fixed excitation wavelength on the plasmon resonance of the NPs aggregates. We use as test molecule rhodamine 6G and the excitation wavelength was of 514 nm.

2 Experimental

2.1 Reagents

Tetrachloroauric acid (HAuCl $3H_2O$), sodium citrate ($HOC(COONa)(CH_2COONa)_2{\cdot}2H_2O$), deionized water, tetraethyorthosilicate ($Si(OC_2H_5)_4$, TEOS), 3-aminopropyl-trimethoxysilane (APTMS), 3-(trimethoxy-silyl) propyl-methacrylate (MPTMS), ammonium hidroxide (NH_4OH) and rhodamine 6G ($C_{28}H_{31}N_2O_3Cl$) ethanol (CH_3CH_2OH) were used as received for sample preparation and SERS characterization. All chemical products were purchased from Sigma-Aldrich. Silicon wafers (SW) of 1 cm^2 and orientation $\langle 100 \rangle$, resistivity 0.01–0.02 $\Omega\,cm$ and thickness of 500–550 μm were purchased from Silicon Valley.

2.2 Synthesis of gold nanoparticles

1 mL of tetrachloroauric acid (1 mM) was dissolved in 20 mL of deionized water. This solution was boiling under stirring for 10 min. Then, 25 mg of sodium citrate was added to the solution that was stirred for 30 min. The solution underwent a series of color changes and finally turning into wine red colloidal suspension [24].

2.3 Synthesis of silica particles

A solution of 10 mL ethanol, 3 mL of water and 0.75 mL of ammonium hydroxide were stirred at room temperature and then 1.2 mL of TEOS was added dropwise into the solution. After 3 h of reaction, the silica particles were centrifuged at 3000 rpm for 30 min and rinsed several times [25].

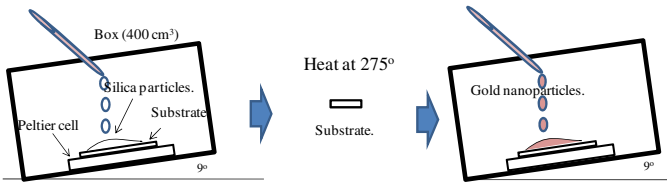

Fig. 1. (Color online) Schematic representation of experimental setup used to obtain aggregates of Au NPs using the colloidal crystal template.

2.4 Assembly of Au NPs aggregates templated by colloidal crystal

The experimental setup consists of a Peltier cell with a temperature controller surrounded by a small plastic box to keep out external air flow and contamination, see Figure 1. The system is tilted 9° and temperature inside the box was kept at 17 °C. The silicon substrate (SW) was cleaned with H_2SO_4 and rinsed with deionized water and ethanol. A droplet (20 μL) of silica particles suspension is spread on the SW substrate. Since the substrate is tilted, a thin water film was formed while the residual water forms a droplet at the lower side of the substrate. Evaporation of water starts from the top of the sample on a horizontal border where evaporation takes place, and moves to the bottom until substrate is completely dried. Evaporation process promotes colloidal crystal arrangement of silica particles in the SW surface. The dried SW substrate was annealed for 3 h at 275 °C to improve crystallinity and eliminate the residual solvent. An aliquot of 10–40 μL of gold solution ($3.5 \times 10^8 - 1.418 \times 10^9$ nanoparticles) was deposited onto the colloidal crystal template and dried under the same experimental condition.

2.5 Silica particles decorated with Au NPs

Silica particles were functionalized with APTMS and MPTMS in different relations (5:95, 30:70 and 50:50). The treatment produces a silica particle surface terminated with amine and methyl groups. Organosilane-coated silica particles were mixed with a suspension of Au NPs leading to a selective adsorption on the silica particle surface. Au NPs are attached on amine terminate groups, while regions with methyl terminated were used as spacers to control their agglomerations [26].

3 Results and discussion

3.1 Au NPs characterization

The particle size was measured by TEM (JEM 1230 JEOL). The average size was 15 ± 3 nm obtained by measuring more than 500 nanoparticles. Figure 2 shows the plasmon resonance for these nanoparticles, while the inset shows a typical TEM image.

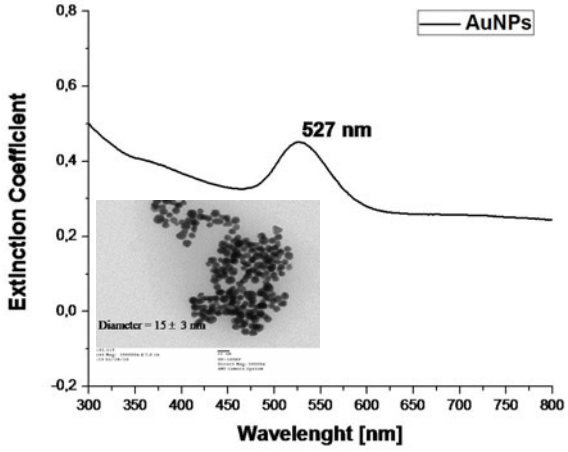

Fig. 2. Plasmon resonance of Au NPs solution centered at 527 nm. The inset shows a typical TEM image.

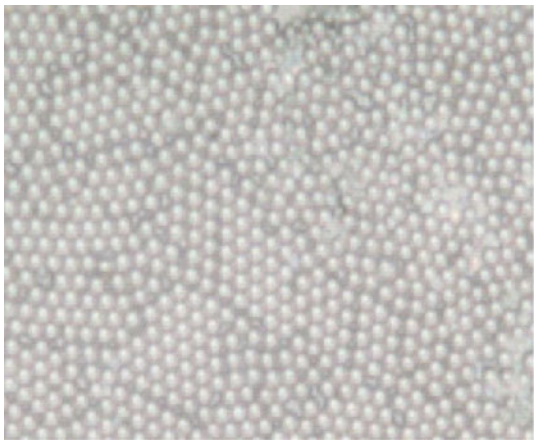

Fig. 3. (a) Optical microscope image of colloidal crystal of silica used as a template, the size of image is ∼50 μm × 40 μm. (b) SEM image of Au NPs aggregates obtained during the deposition of gold nanoparticles in the template.

3.2 Aggregates characterization

Figure 3 shows an optical microscope image of colloidal crystal on SW surface. As expected, the array of silica particles was regular with an average particle size of ∼1.3 μm. Au NPs were deposited into the interstices of silica array forming aggregates. The size of aggregates depends on the silica particle size and the Au NPs concentration on the solution deposited on silica particles array. The size increment of aggregate induces a red-shift of the plasmon resonance band as is shown in Figure 4. The maximum red-shift observed as a function of Au NPs concentration was approximately 23 nm respect to the plasmon resonance peak in Figure 2.

3.3 Silica decorated with Au NPs

Figure 5 shows a typical TEM picture of 1.3 μm silica core decorated with Au NPs. Distribution of gold nanoparticles grafted over the silica surface depends on the

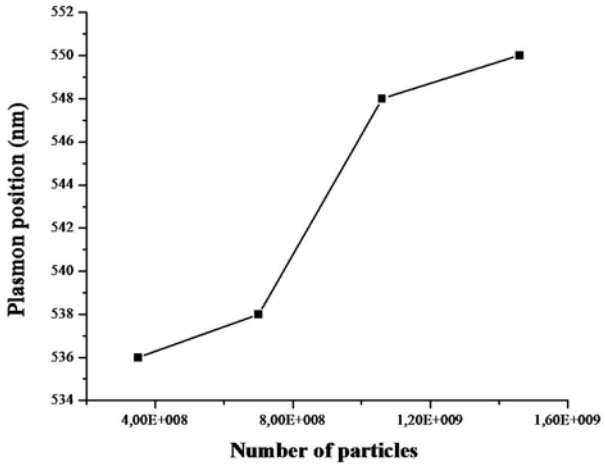

Fig. 4. Red-shift of plasmon resonance band as a function of aggregate size.

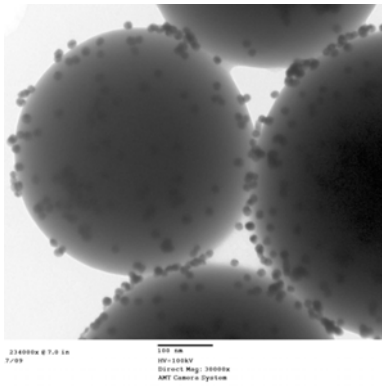

Fig. 5. TEM image of silica core decorated with Au NPs.

APTMS:MPTMS volume ratio used during the functionalization of silica particle. Contrary to other works [22], this methodology allows the control the density of Au NPs adsorbed onto silica particle by a simple variation of APTMS:MPTMS ratio, an increment of Au NPs density attached on silica surface was observed by changing the APTMS:MPTMS ratio from 5:95 to 50:50, such increment produces hot spot sites, and induces a red-shift of the plasmon resonance peak, as is observed in Figure 6. The shifting is the result of the plasmon resonance originated by the decreasing of distance between nanoparticles grafted on silica particle at high Au NPs densities. The maximum shift of ∼16 nm respect to individual plasmon band was observed for particles functionalized with 50:50 APTMS:MPTMS ratio. This behavior is due to the formation of Au NPs aggregates on silica arrays.

3.4 Surface enhanced Raman scattering (SERS)

Au NPs aggregates formed on the interstice of colloidal silica template and gold decorated silica, both deposited on SW substrate, were used to enhance the Raman signal of rhodamine 6G (R6G) at concentrations as lower as

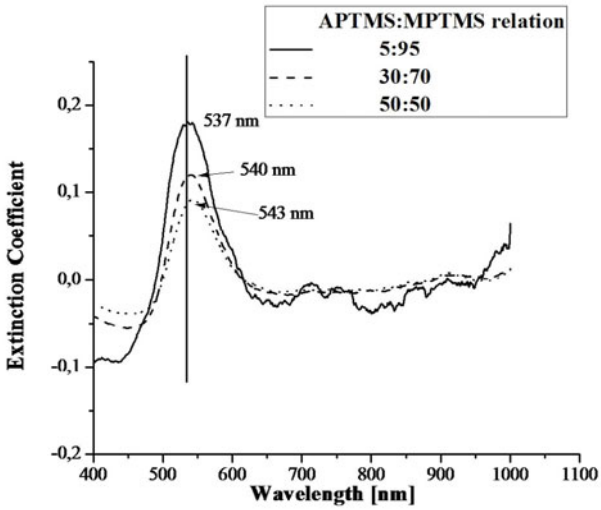

Fig. 6. Red-shift of resonance plasmon by increasing Au NPs concentration attached to silica core.

10^{-6} M. No Raman signal was observed for this concentration without the presence of Au NPs. The adsorption of R6G molecules onto gold aggregates and decorated silica were made by depositing a drop ($\sim$20 μL) of rhodamine on an area $\sim$1 cm^2 and dried at room temperature. Raman signal was recorder by using a Renishaw micro Raman system with 100× objective (Leica, N.A 0.85) at the excitation wavelength of 514 nm. The incident intensity is about 20 mW on the sample, and the integration time was of 10 s. Regions investigated with this objective have an area of $\sim$1 μm^2. Signal without gold nanoparticles was measure at a concentration of 1×10^{-2} M and used as reference. SERS signal was produced by 1.52×10^5 R6G molecules and reference by 1.88×10^7 molecules.

3.5 SERS on gold nanoparticles aggregates

The Raman spectrum for R6G deposited on aggregates of gold nanoparticles template-by the colloidal silica crystal is shown in Figure 7a. Characteristic Raman signal at 1646 cm^{-1} for different aggregates size are shown in the inset of Figure 7a, where is observed that band positions do not change with the aggregates size. The same behavior was observed in different parts of the same substrate (data not showed here), suggesting a homogeneous distribution of aggregates along the SW surface.

The Raman signal of R6G in these colloidal silica templates is increased as the size of Au NPs aggregate decreases. This is shown in Figure 7a for four aggregates sizes, corresponding to 3.5×10^8, 7×10^8, 1.063×10^9 and 1.41×10^9 particles deposited on silica template and called SG1, SG2, SG3, and SG4, respectively. The maximum signal is observed for sample SG1 and the minimum for sample SG4 (Fig. 7b). The behavior for sample SG1 is attributed to the fact that the plasmon resonance of Au aggregates and the absorption wavelength of test molecule are closely in resonance with the excitation wavelength for the sample, which is the opposite case for SG4. Even if the

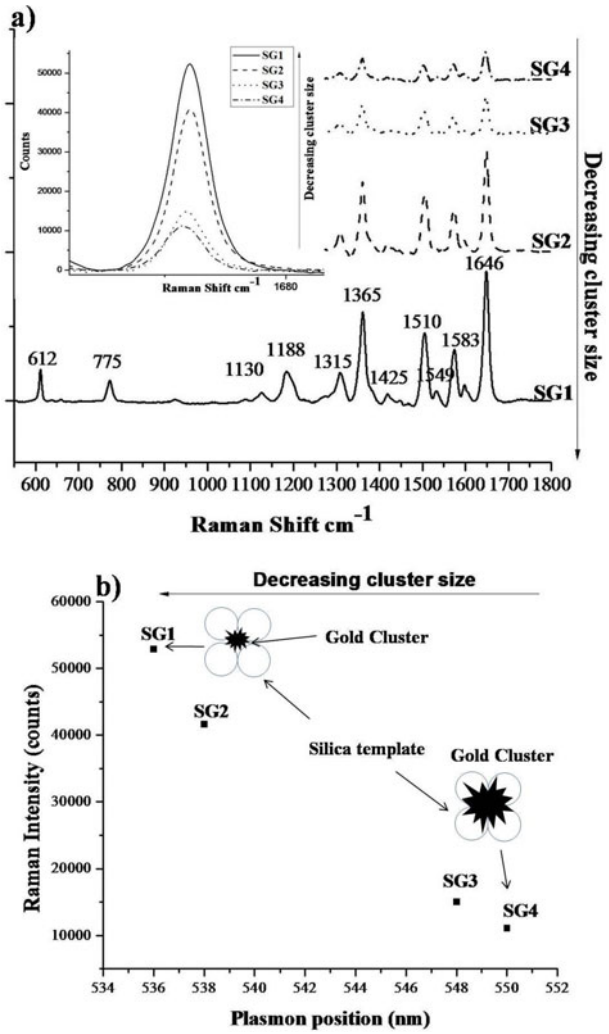

Fig. 7. (a) R6G SERS spectra of Au NPs aggregates templated by a colloidal silica crystal. (b) Behavior of intensity of Raman signal of R6G for different sizes of aggregates.

excitation wavelength is not completely in resonance with each plasmon band, an enhancement factor (EF) of $\sim 10^6$ was obtained with SG1. Such EF is two orders of magnitude higher than that obtained for a porous thin film of gold fabricated in a similar way than our aggregates and reported recently [27]. Furthermore, it is $\sim 10^2$ higher than the response obtained with a substrate with dispersed Au NPs (no agglomeration). However, as the size of aggregates increases (sample SG2, SG3, and SG4) the plasmon resonance band moves away from resonance with the excitation source. As a consequence, sample SG4 have the lowest Raman enhancement, being five times lower than that obtained for SG1. Such strong difference remarks the importance of Au NPs agglomeration size that defines its plasmon resonance. The EF is based on the equilibrium between the HS formation and the plasmon band position of the NPs agglomeration. This behavior is shown in Figure 7b where the maximum enhancement of Raman signal occurs when the plasmon resonance of aggregates is close to wavelength of the excitation laser.

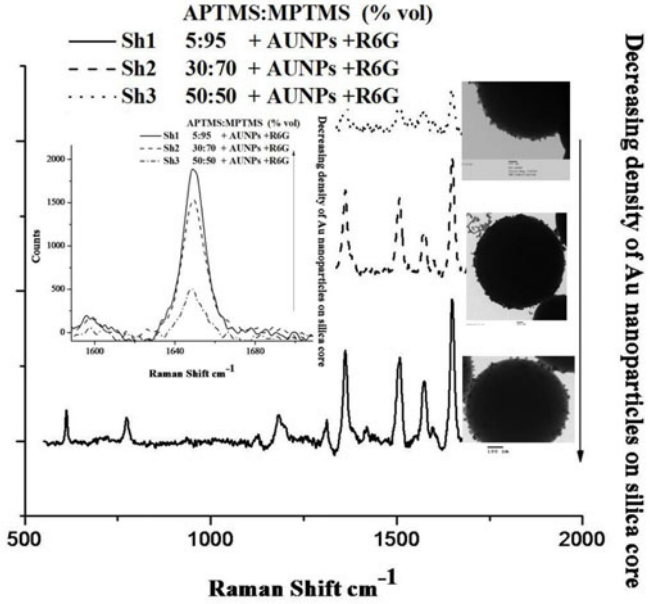

Fig. 8. R6G SERS spectra of decorated silica for three different densities of Au NPs adsorbed on silica surface.

3.6 SERS from silica decorated with Au NPs

Figure 8 shows the Raman spectrum of rhodamine 6G deposited on three different samples of decorated silica system. As observed, the Raman signal decreases from sample Sh1 to sample Sh3. The former one corresponds to the sample with the lowest density of Au NPs obtained from APTMS:MPTMS ratio of 5:95. This result shows that a variation in the APTMS:MPTMS ratio produces also a variation in the NPs aggregates, therefore this ratio not only defines the distance separation between NPs on the silica particle, but also the NPs aggregates when these particles form arrays on the SW. The reduction of Raman signal for larger content of MPTMS, and then high concentration of Au NPs on the silica particle, forms larger aggregate size and the aggregate plasmon band is red-shifted. The Raman signal intensity of 1646 cm^{-1} peak was measured at different densities of attached Au NPs, and its values are shown in the inset of Figure 8. The calculated EF was $\sim 8.8 \times 10^4$ for Sh1 and 2.3×10^4 for Sh3.

Figure 9 shows the Raman signal intensity as a function of plasmon position peak of the NPs aggregates for samples Sh1, Sh2, and Sh3. As was discussed above for the aggregates formed on the silica templates, the plasmon resonance band was also red-shifted as the agglomerate size increases with the MPTMS content, and the resonance with excitation wavelength was also reduced, producing a decreasing the Raman signal intensity. However, these systems can produce an enhancement of Raman signal though the excitation wavelength does not match very well with the position of plasmon resonance of each sample.

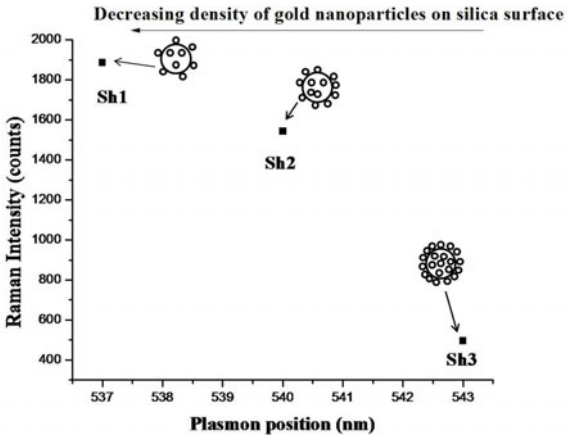

Fig. 9. Behavior of Raman signal intensity of R6G for different densities of Au NPs on silica surface.

4 Discussion

Two experimental approaches for the preparation of Au NPs aggregates have been presented. Template of silica particles and Au NPs decorated silica particles provide systematic procedure for the preparation of size-controlled aggregates. The EF was found between 10^4 and 10^6 and it is associated to the generation of HS as a result of the adequate separation between NPs. The agglomeration of NPs increases the HS sites that in turn increase the EF, but an excess of Au NPs gets them closer breaking the condition for optimum enhancement of the electromagnetic field. In addition, an excess of NPs could promote coalescence. The electromagnetic field of agglomerated NPs is coupled resulting on a red-shift of the plasmon resonance. This property could be an advantage because it provides a mechanism to move the plasmon resonance to a position closer to the resonance with the excitation wavelength. In our particular case, plasmon position moves away from resonance producing a decreasing effect on the EF. These results remark the importance of aggregate size control in order to match the plasmon resonance spectrum with excitation wavelength for the detection of low molecular concentration. This matching condition could be maintained by changing the excitation wavelength, which is not always accessible for the common commercial Raman apparatus. However, it is possible to obtain good SERS signal using gold aggregates whose plasmon resonance spectrum partially matches the excitation wavelength.

5 Conclusion

In conclusion, control size agglomeration of Au NPs by using a silica template and decorating silica particles has been demonstrated. The EF was greater for agglomerate prepared with silica template than for the NPs decorated silica particles, as a result of the increase of HS sites. In both cases, the EF diminishes with the excess of NPs; such effect is produced by the red shift of plasmon resonance

band away from resonance with excitation wavelength. The methodologies for SERS substrate preparation are simple, reliable and not too expensive, and moreover produce a high enough enhancement factor for sensing low concentration of analytes.

The financial support of CONCyTEG grant 09-04-K662-072, CONACyT grant 49482, and PROMEP are acknowledged. F. Castillo thanks to CONACYT for the PhD scholarship (221405). Authors thanks to Q.F.B. Ma. de Lourdes González González (IF-UASLP) for technical support in the synthesis of gold and silica particles; M.C. Claudia Elías Alfaro and Ing. Fernando Rodríguez Juárez, from (IMUASLP), for her advising and support on the TEM and SEM characterization of gold and silica particles, and to Miguel Angel Vidal Borbolla from IPICYT, for facilities to use Raman spectrometer.

References

1. S. Nie, S.R. Emory, Science **275**, 1102 (1997)
2. K. Kneipp, Y. Wang, H. Kneipp, L.T. Perelman, I. Itzkan, R.R. Dasari, M.S. Feld, Phys. Rev. Lett. **78**, 1667 (1997)
3. M. Moskovits, Rev. Mod. Phys. **57**, 783 (1985)
4. Hongxing Xu, J. Aizpurura, M. Käll, P. Apell, Phys. Rev. E **62**, 3 (2000)
5. G.C. Schatz, R.P. Van Duyne, Electromagnetic mechanism of surfaceenhanced spectroscopy, in *Handbook of Vibrational Spectroscopy*, edited by J.M. Chalmers, P.R. Griffiths (John Wiley & Sons, Ltd., 2002), pp. 759–774
6. R. Aroca, *Surface-enhanced Vibrational Spectroscopy* (John Wiley & Sons, Chichester, 2006)
7. E.C. Le Ru, P.G. Etchegoin, *Principles of Surface Enhanced Raman Spectroscopy, and related plasmonic effects* (Elsevier, Amsterdam, 2009)
8. E.C. Le Ru, E. Blackie, M. Mayer, P.G. Etchegoin, J. Phys. Chem. C. **111**, 13794 (2007)
9. A. Campion, P. Kambhampati, Chem. Soc. Rev. **27**, 241 (1998)
10. F.J. García-Vidal, J.B. Pendry, Phys. Rev. Lett. **77**, 1163 (1996)
11. J. Grand, M. Lamy de la Chapelle, J.-L. Bijeon, P.-M. Adam, A. Vidal, P. Royer, Phys. Rev. B **72**, 033407 (2005)
12. M.T. Sun, S.B. Wang, Y.J. Liu, Y. Jia, H.X. Xu, J. Raman Spectrosc. **39**, 402 (2008)
13. J.R. Lombardi, R.L. Birke, J. Chem. Phys. **126**, 244709 (2007)
14. L. Gunnarsson, E.J. Bjerneld, H.X. Xu, S. Petronis, B. Kasemo, M. Käll, Appl. Phys. Lett. **78**, 802 (2001)
15. Wei Wang, Zhipeng Li, Baohua Gu, Zhenyu Zhang, Hongxing Xu, ACS Nano **3**, 3493 (2009)
16. A.M. Michaels, J. Jiang, L.J. Brus, Phys. Chem. B **104**, 11965 (2000)
17. A.M. Schwartzberg et al., J. Phys. Chem. B **108**, 19191 (2004)
18. K. Kneipp, H. Kneipp, R. Manoharan, E.B. Hanlon, I. Itzkan, R.R. Dasari, M.S. Feld, Appl. Spectrosc. **52**, 12 (1998)
19. Rongchao Jin, Angew. Chem. Int. Ed. **49**, 2826 (2010)
20. J. Zhang et al., J. Phys. Chem. B **108**, 19191 (2004)
21. W. Wang et al., Anal. Chim. Acta **567**, 121 (2006)
22. W. Wang et al., Anal. Chim. Acta **567**, 121 (2006)
23. B. Yan et al., ACS Nano **3**, 1190 (2009)
24. J. Turkenvich, P.C. Stevenson, J. Hillier, Discuss. Faraday Soc. **11**, 55 (1951)
25. D. Kandpal, S. Kalele, S.K. Kulkarni, Pramana J. Phys. **69**, 2 (2000)
26. S.L. Westcott, S.J. Oldenburg, T.R. Lee, N.J. Halas, Langmuir **14**, 19 (1998)
27. P.M. Tessier, O.D. Velev, A.T. Kalambur, J.F. Rabolt, A.M. Lenhoff, E.W. Kaler, J. Am. Chem. Soc. **122**, 9554 (2000)